Automated Pulsed Eddy Current Method for Detection and Classification of Hidden Corrosion

Article · January 2005

CITATIONS
3

READS
162

5 authors, including:

Zheng Liu
University of British Columbia - Okanagan
232 PUBLICATIONS **4,480** CITATIONS
SEE PROFILE

David S. Forsyth
TRI Austin
184 PUBLICATIONS **826** CITATIONS
SEE PROFILE

Abbas Fahr
National Research Council Canada
152 PUBLICATIONS **926** CITATIONS
SEE PROFILE

Proc. Vth International Workshop, Advances in Signal Processing for Non Destructive Evaluation of Materials
Québec City (Canada),2-4 Aug. 2005. © X. Maldague ed., É. du CAO (2006), ISBN 2-9809199-0-X

Automated Pulsed Eddy Current Method for Detection and Classification of Hidden Corrosion

M. S. Safizadeh, Z. Liu, C. Mandache, D. S. Forsyth, and A. Fahr

Structures, Materials & Propulsion Laboratory, Institute for Aerospace Research, National Research Council Canada, Building M-14, 1200 Montreal Rd., Ottawa, Ontario, Canada

Abstract

Corrosion has an important effect on the structural integrity of aging aircraft components, and an automatic and effective method of corrosion detection and classification can help to ensure the safe operation of a transportation system. Pulsed eddy current (PEC) has been shown to effectively characterize hidden corrosion in aircraft fuselage lap joints. However, two noise sources in the form of probe lift-off and interlayer gap can cause false indications or inaccuracies in quantification.

This paper describes the development of a modular architecture for analysis of PEC data to enable automatic characterization of hidden corrosion in a typical aircraft fuselage multi-layer structure. The goal of this study was to develop a software tool to detect and distinguish between first layer and second layer corrosion damage.

This investigation is a follow on to previous work that applied time-frequency analysis of PEC signals to provide specific visual patterns related to the interlayer gap, lift-off, and material loss. In the present work, the authors have investigated the time-frequency analysis of PEC signals along with feature extraction and classification to automatically characterize and determine the location of material loss in a two-layer structure.

1. Introduction:

Recent advances in the pulsed eddy current technique have shown the potential to detect and characterise hidden corrosion in multi-layer aircraft structures such as lap splices [1,2].

In PEC, the probe's driving coil is excited by repeated pulses. For every pulse, the response signal is measured with a sensor, which may be the driving coil, another

coil, or a Hall or GMR sensor. By sampling the time-domain response using a high-speed digitiser, the probe response is effectively captured over a wide range of frequencies within a single measurement. This allows inspection of the entire depth of the specimen with just one pulse.

The most common features used in the analysis of PEC signals for detection and characterization of material loss due to corrosion in multi-layer structures are the amplitude, time-to-peak or time-to zero-crossing. However, these features are not sufficient for discriminating signals due to corrosion –induced metal loss from unwanted noise. Two of the most important noise sources in lap joint inspections are the variation in probe lift-off and interlayer gap due to change in paint or adhesive thickness, and corrosion pillowing. Previous work of the authors [3] has shown that the time-frequency analysis of pulsed eddy current signals provides visual discrimination between the simultaneous occurrence of material loss and changes in interlayer gap or lift-off. However, this method cannot currently be readily used because of difficulties in calibration and the lack of an automatic detection and classification system.

This paper presents an automated pulsed eddy current method capable of detecting and classifying the material loss due to corrosion, and determining its location in a two-layer structure.

2. Principal of method:

Conventional pulsed eddy current techniques for corrosion detection and characterization rely on the analysis of signal features that are represented as c-scan images. Only experienced operators are able to perform full evaluation of pulsed eddy current c-scan images. Increasing emphasis on reliability and demand for tools that can assist operators have motivated research for an automated pulsed eddy current detection and classification system.

The automatic pulsed eddy current detection and classification system developed in this work includes three modules: a time-frequency analysis module, feature extraction module, and classification module; as shown in Figure 1.

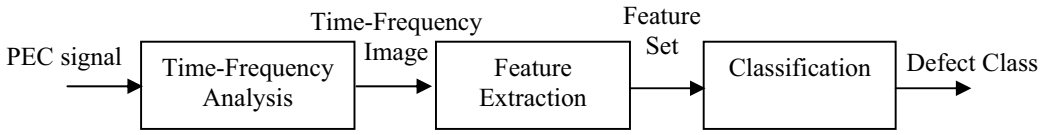

Figure 1: Modular architecture for the proposed pulsed eddy current system.

Details about each module are described in the following.

2.1. Time-Frequency Module

Time-frequency analysis provides a three-dimensional representation of signals in time-frequency-amplitude space, but usually, the projection of this three-dimensional representation is shown in the two-dimensional time-frequency plane with grey scale representing the amplitude.

There are several possible time-frequency distributions; however, we will focus only on the Wigner-Ville distribution (WVD) that is most commonly used.

The Wigner-Ville distribution of a signal $s(t)$ is defined as [4]:

$$WVD_s(t,\omega) = \int_{-\infty}^{\infty} s(t+\tau/2)s^*(t-\tau/2)e^{-j\omega\tau}d\tau \tag{1}$$

where $s(t)$ is a continuous complex signal, τ is a time shift variable and the asterisk denotes the complex conjugation. The discrete-time and discrete-frequency version of equation (1) is given by [5]:

$$WVD_s(n,\pi m/M) = 2\sum_{k=-M/2+1}^{M/2} p(k)s(n+k)s^*(n-k)\exp(-j2\pi mk/M) \qquad m = 0,1,2,\ldots,M-1 \tag{2}$$

where $p(k)$ is the window function such as Hamming, Hanning, or rectangle with the length M centred about n.

The WVD has a number of desirable mathematical properties such as time and frequency marginal conditions, instantaneous frequency, time shift, frequency shift, and time and frequency support properties. Despite the desirable properties of the WVD, it has two major draw-backs: it is not necessarily non-negative and it is a bilinear function producing interferences or cross terms for multi-component signals. In practical applications, the WVD requires some smoothing in order to suppress the cross terms.

2.2. Feature Extraction Module

Feature extraction is crucial for pattern recognition systems. The number of features determines the measurement cost and a well-defined feature set plays an important role in the accuracy and efficiency of the subsequent processing.

The output of the time-frequency analysis module is the WVD representation of the pulsed eddy current signals, which are images with a large amount of redundant information. To improve computational efficiency, it is vital to reduce the number of parameters (inputs) in the classifier. Two different feature extractors are used and compared in this study.

One well known linear feature extractor is principal component analysis (PCA) [6]. PCA is a method of identifying patterns in data (the time-frequency images of the PEC signals in our case), and expressing the data in such a way as to highlight their similarities and differences.

PCA computes the m largest eigenvectors of the $d \times d$ covariance matrix of the $n \times d$-dimensional patterns. The linear transformation is defined as:

$$Y = HX \tag{3}$$

where X is the given $n \times d$ pattern matrix, Y is the derived $n \times m$ $(m < d)$ pattern matrix, and H is the $d \times m$ matrix of linear transformation whose columns are the eigenvectors. Since PCA only retains the most expressive features (eigenvectors with the largest eigenvalues), it effectively reduces the number of dimensions without much loss of information.

Let each WVD image be a $N \times N$ matrix. This matrix can be expressed as a N^2-dimensional vector where the rows of pixels in the image are placed one after the other to form a one-dimensional image.

$$WVD = (w_{11} w_{12} \ldots w_{1N} w_{21} \ldots w_{NN}) \tag{4}$$

The values in the vector are the intensity values of the image, possibly a single greyscale value. All the WVD image vectors are then put in one matrix:

$$X = \begin{pmatrix} \text{Image Vector 1} \\ \text{Image Vector 2} \\ \vdots \\ \text{Image Vector n} \end{pmatrix} \tag{5}$$

which gives us a starting point for our PCA analysis. Since all the vectors are N^2 dimensional, we will get N^2 eigenvectors. Once we have performed PCA, we obtain the original data mapped into the axis corresponding to the eigenvectors. In practice, we are able to leave out some less significant eigenvectors. In our case, two eigenvectors that correspond to the two largest eigenvalues are chosen for investigation. This choice of eigenvectors permits a visual examination of the data.

Another feature extractor which has been examined is the moments in time and frequency of a time-frequency representation. Since the time-frequency image describes the evolution with time of the frequency content of the signal, the extraction of information has to be done with care from the knowledge of these properties. The first order moments of a Wigner-Ville distribution in time and in frequency are defined as:

$$\langle \omega \rangle_t = \frac{\int_{-\infty}^{+\infty} \omega \, WVD(t,\omega)\, d\omega}{\int_{-\infty}^{+\infty} WVD(t,\omega)\, d\omega}$$
$$\langle t \rangle_\omega = \frac{\int_{-\infty}^{+\infty} t \, WVD(t,\omega)\, dt}{\int_{-\infty}^{+\infty} WVD(t,\omega)\, dt} \qquad (6)$$

Equation 6 describes the averaged position and spread in time and frequency of the signal. For a Wigner-Ville distribution, the first order moment in time also corresponds to the instantaneous frequency, and the first order moment in frequency to the group delay of the signal. In this study, the first key feature is $\langle \omega \rangle_{t=0}$ and the second one is $\langle t \rangle_{\omega=0}$.

The output from the feature extraction module is an optimal set of features extracted from WVD images that are then fed to the classification module.

2.3. Classification Module

The role of the classification module is to classify or describe observations relying on the extracted features. The classification scheme is usually based on the availability of a set of patterns that have already been classified or described. This set of patterns is termed the training set and the resulting learning strategy is characterised as supervised. Learning can also be unsupervised, in the sense that the system is not given a priori labelling of patterns, instead it establishes the classes itself based on the statistical regularities of the patterns.

The classification scheme usually uses one of the following approaches: template, statistical (or decision theoretic), syntactic (or structural), or neural. In template matching, a template or a prototype of the pattern to be recognized is available. Statistical pattern recognition is based on statistical characterisations of patterns, assuming that the patterns are generated by a probabilistic system. Structural pattern recognition is based on the structural interrelationships of features. Neural pattern recognition employs the neural computing paradigm that has emerged with neural networks.

In our case, a Fisher's linear discriminant is implemented to take care of the last processing step that consists of decision making regarding the defect class. This classifier minimizes the mean squared error (MSE) between the classifier output and the desired labels. It projects high dimensional data onto a line and performs classification in this one-dimensional space. The projection maximizes the distance between the means of the two classes while minimizing the variance within each class. Details about this classifier and other classifiers can be found in [7].

3. Experiments:

The PEC instrumentation used for this work consisted of a pulse generator, a pre-amplifier, an XY positioning robot and a computer-controlled data acquisition system. A schematic of this setup is shown in Figure 2. The driver coil is excited with a 12 volt, 500 μs long step function triggered upon the probe's arrival at a point of acquisition. The signal is measured as a time-based voltage drop across a resistor in series with the pick-up coil, and fed into a low-noise amplifier. This signal response in the time domain is often called an A-scan. The scanning and data acquisition operations are controlled by the Utex Winspect™ software package. Although the system can accommodate several probe-coil configurations, only the sliding probe arrangement was used in this study. The probe consists of two adjacent coils in driver/pickup configuration.

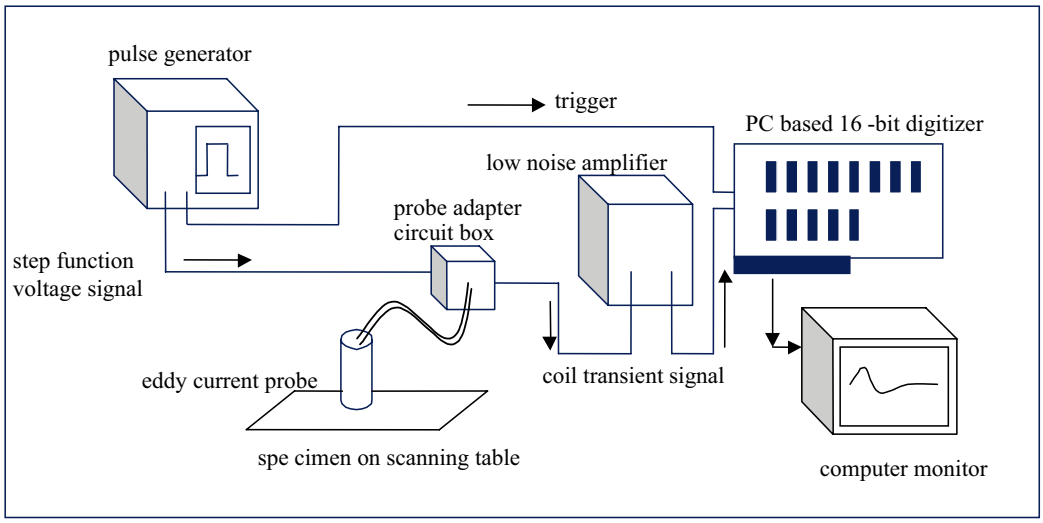

Figure 2: A schematic illustration of the PEC apparatus used in this study.

A test specimen was constructed to simulate a two-layer 0.040"/0.040" aluminium alloy lap splice, as shown in Figure 3. Material loss due to corrosion was simulated by milled areas.

The specimen was scanned at a 1 mm resolution. The signals in each region of interest were captured with 1 MHz sampling frequency. It is the reference subtracted signal, rather than the raw signal, that is analysed when evaluating the condition of the lap splice. The reference signal was taken as the average of all A-scan signals in the region away from flaws. Subsequently, the reference signal was subtracted from those of interest, resulting in a set of reference subtracted signals. These represent the perturbations due to metal loss or other abnormal conditions. Hence forth, these signals will be referred as simple PEC signals.

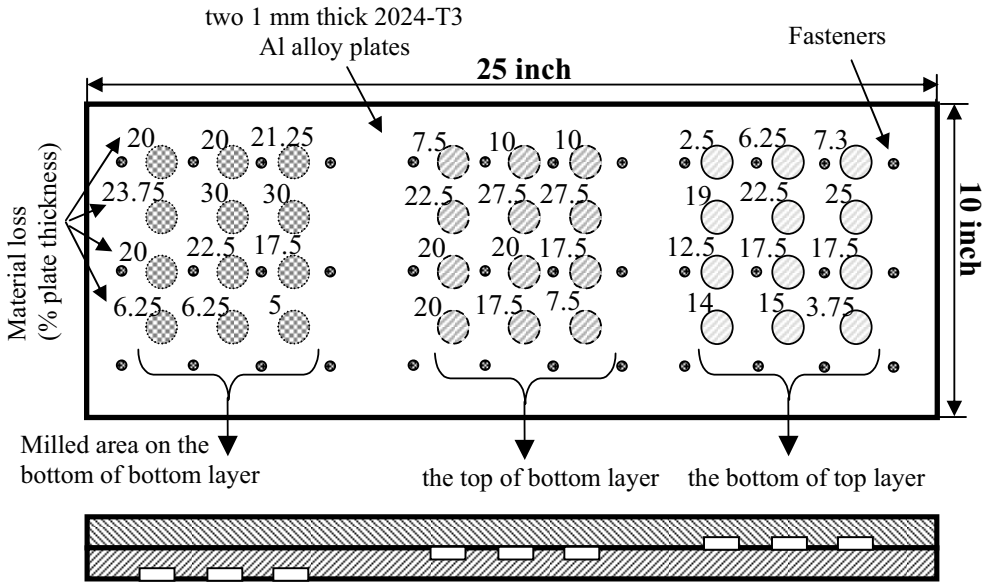

Figure 3: The configuration of the test specimen used in this study.

4. Results and Discussion:

The subtracted defect signatures are fed to the Wigner-Ville Distribution (WVD) computer block to obtain the corresponding WVD images. These WVD images are presented to the feature extractor block for optimal feature extraction. Both feature extractors explained in section 2.2 (PCA and the first order moments of WVD) have been applied to the WVD images and the key features obtained from each extractor have been sent to the classifier separately.

Six different defect classes are considered to test the performance of the proposed method. There are three categories for the location of defects: bottom of top layer (BOT), top of bottom layer (TOB) and bottom of bottom layer (BOB). Each category is divided in two classes: defect with less than 10% of the layer thickness and defect with more than 10% of the layer thickness. The extracted features corresponding to the six simulated defect signatures are fed to the classifier for training. Every training input data is labelled with its corresponding class as indicated in Table 1.

Table 1: List of defect classes and training data set

Defect Class	Training Data
BOT <10%	bot 2.5% & bot 7.5%
BOT >10%	bot 17.5% & bot 25%
TOB <10%	tob 7.5% & tob 10%
TOB >10%	tob 17.5% & tob 27.5%
BOB <10%	bob 5% & bob 6.25%
BOB >10%	bob 20% & bob 30%

The classifier uses these training data to provide the decision boundary. Then, the trained classifier assigns the test data to one of the classes under consideration based on the measured features. Since two different feature extractors were used, the classification process was performed for each of them separately. To get a better sense of the results, the defect classes determined by the classifier for each test data are shown in Figure 4.

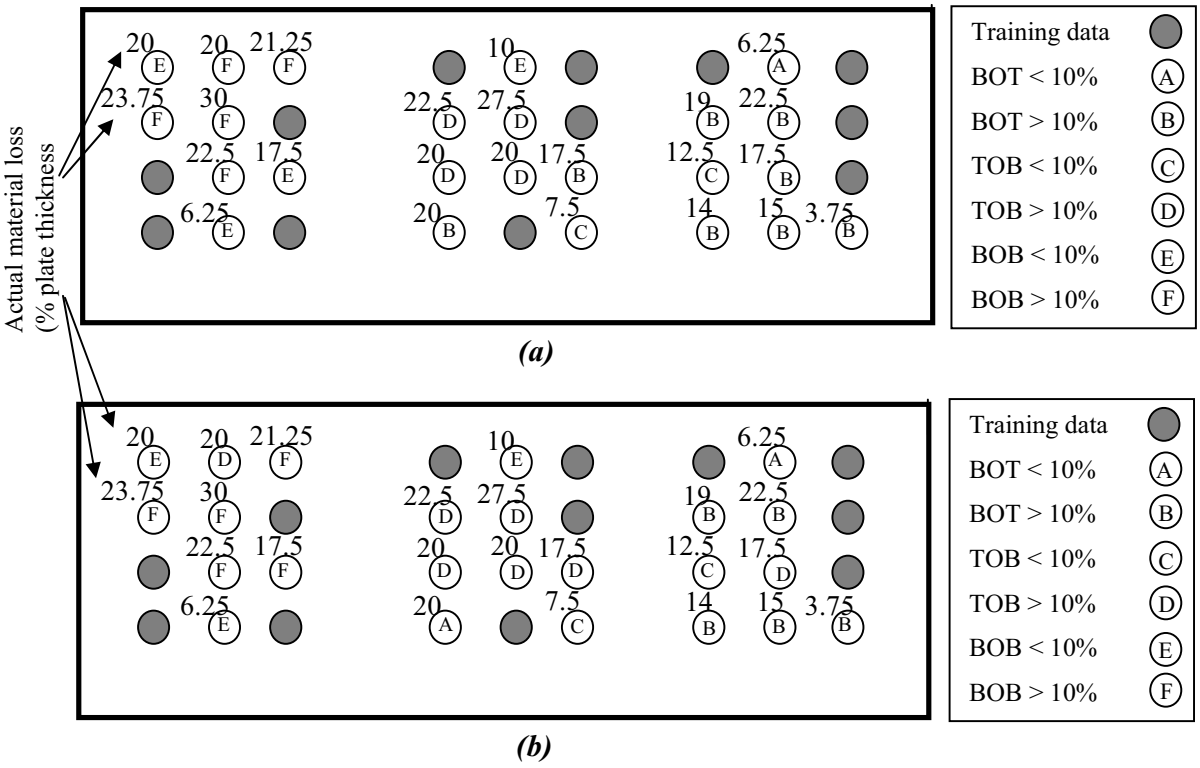

Figure 4: Estimated material loss by classifier using (a) PCA and (b) the first moment of WVD as a feature extractor

Table 2 summarizes the defect classes, the actual material loss and the evaluation for each test data.

Table 2: Comparing actual material losses with defect classes obtained by classifier

Actual Material Loss	Defect Class (using PCA)	Evaluation (using PCA)	Defect Class (using MOM)	Evaluation (using MOM)
BOT 3.75%	BOT > 10%	False	BOT > 10%	False
BOT 6.25%	BOT < 10%	True	BOT < 10%	True
BOT 12.5%	TOB <10%	False	TOB <10%	False
BOT 14%	BOT >10%	True	BOT >10%	True
BOT 15%	BOT >10%	True	BOT >10%	True

BOT 17.5%	BOT > 10%	True	TOB > 10%	False
BOT 19%	BOT > 10%	True	BOT > 10%	True
BOT 22.5%	BOT > 10%	True	BOT > 10%	True
TOB 7.5%	TOB < 10%	True	TOB < 10%	True
TOB 10%	BOB < 10%	False	BOB < 10%	False
TOB 17.5%	BOT > 10%	False	TOB > 10%	True
TOB 20%	TOB > 10%	True	TOB > 10%	True
TOB 20%	TOB > 10%	True	TOB > 10%	True
TOB 20%	BOT > 10%	False	BOT < 10%	False
TOB 22.5%	TOB > 10%	True	TOB > 10%	True
TOB 27.5%	TOB > 10%	True	TOB > 10%	True
BOB 6.25%	BOB < 10%	True	BOB < 10%	True
BOB 17.5%	BOB < 10%	False	BOB > 10%	True
BOB 20%	BOB >10%	True	TOB > 10%	False
BOB 20%	BOB < 10%	False	BOB < 10%	False
BOB 21.25%	BOB > 10%	True	BOB > 10%	True
BOB 22.5%	BOB > 10%	True	BOB > 10%	True
BOB 23.75%	BOB > 10%	True	BOB > 10%	True
BOB 30%	BOB > 10%	True	BOB > 10%	True

It is clear from Table 2 that in most cases the classifier gives a correct response except when the material loss size is very close to the limit of the class such as 10 or 12.5% material loss. In some cases, the training data do not well represent the classes and are far from the limit of the class. In such a case, the classifier cannot accurately define the boundary of classes.

On the other hand, the results from the two feature extractors used in this study give the same number of false responses. It is very difficult to arrive at a conclusion regarding the performance of these two feature extractors.

There are some error sources that must be addressed. The extractor block only provided two features for each WVD image to permit a visual examination of the data. The PCA analysis can extract more features to better represent the WVD images. In case of the first order moment of WVD, the extraction of the second order moment of WVD can also be interesting to consider because it contains some additional information about the given time-frequency representation. In other words, the loss of information brought on by the PCA analysis or the moment of WVD can be kept at a minimum.

The number of training samples plays an important role in the classification performance. In practice, the error rate of a recognition system is a function of the number of training and test samples. The error rate becomes smaller and smaller as the ratio of the number of training samples per class to the dimensionality of the feature vector gets larger and larger. In this case, there were only two data per class for training the classifier. Despite the small number of training data, the results were good. A large number of training data can significantly improve the performance of the classifier. It is also noted that the classifier approach adopted

in the classification block is the simplest classifier. Using a nonlinear classifier or a neural network classifier may better define the decision boundaries and consequently reduce the error, but they are very sensitive to the number of training data.

5. Conclusion:

In this paper, an automated detection and classification system based on the pulsed eddy current measurements for automatic characterization of material loss in a typical aircraft fuselage multi-layer structure has been developed. The application of joint time-frequency analysis and pattern recognition to pulsed eddy current signals provides an automatic defect classification system and expands the role of the pulsed eddy current technique in the characterization of hidden corrosion in multi-layer lap splice specimens.

6. Reference:

1. Lepine B.A., Wallace B.P., Forsyth D.S., and Wyglinski A., " *Pulsed eddy current method developments for hidden corrosion detection in aircraft lap splices.*" Proceedings of the 1st Pan-American Conference for Nondestructive Testing, Sept 1998.

2. Bieber J.A., Tai C., and Moulder J.C., " *Quantitative assessment of corrosion in aircraft structures using scanning pulsed eddy current.*" Review of Progress in Quantitative Nondestructive Evaluation, 17, 1998, PP. 315-322.

3. Safizadeh M.S., Lepine B.A., Forsyth D.S., and Fahr A., " *Time-Frequency Analysis of Pulsed Eddy Current Signals*," Journal of Nondestructive Evaluation, Vol.20, No. 2, PP. 73-86, June 2001.

4. Cohen L., "Time-Frequency Analysis," Prentice Hall, 2000

5. Classen T.A.C.M., Mecklenbrauker W.F.G., "The Wigner Distribution – A Tool for Time-Frequency Signal Analysis", Philips J. Res., 35, 1980, PP. 217-250, 276-300, 372-389.

6. O'Connel M.J., "Search Program for Significant Variables", Computer Physics Communications, Vol. 8, No. 1, August 1974.

7. Jain A.K. Dulin R.P.W. and Jianchang M., "Statistical Pattern Recognition: A Review", IEEE Transaction on Pattern Analysis and Machine Intelligence, Vol. 22, No. 1, January 2000.